Ta and N modulated electronic, optical and photocatalytic properties of TiO$_2$

Ya Fei Zhao, Can Li *, Ji Yuan Hu, Yin Yan Gong, Leng Yuan Niu, Xin Juan Liu

Institute of Coordination Bond Metrology and Engineering, School of Materials Science and Engineering, China Jiliang University, China

A B S T R A C T

Bond relaxation and the associated electronic energies mediate the properties of a substance, and therefore, doping could be the effective means for such purpose. With the aid of first principle calculations and experimental observations, we examine four co-doped specimens (Ta–N^1, Ta–N^2, Ta–N^3, Ta–N^4) with different Ta and N co-doped positions, and show that Ta or N addition could modulate the electronic, optical and photocatalytic responses of TiO$_2$ for photocatalysts applications. Results show that, Ta–O bonding not only reduces the electronic transition energies but also increased the carrier mobility of impurity level in Ta-doped and Ta–N^2, Ta–N^3, and Ta–N^4 co-doped TiO$_2$ specimens, while the impurity level disappears and the band gap reduces by 0.46 eV in Ta–N^1 co-doped specimen due to the forming Ta–N bonding. Most strikingly, Ta–N co-doped TiO$_2$ have twofold photocatalytic ability better than pure TiO$_2$ under visible light excitation.

© 2015 Elsevier B.V. All rights reserved.

1. Introduction

The photocatalyst titania (TiO$_2$) has been studied widely due to its superior efficient properties, such as inexpensive, chemically stable, nontoxic and high photocatalytic activity [1–4]. However, its practical application has been limited by its large intrinsic band gap and high recombination rate of electron–hole pairs [5]. Thus, TiO$_2$ can only absorb the ultraviolet (UV) part of the solar spectrum (about 5% of the solar energy) [6–9]. In order to enhance the effective utilization of TiO$_2$ based photocatalyst under solar spectrum, it is of great importance to enhance the utilization rate of visible light that accounts for 45% energy of the solar spectrum [10–14].

There are three key concerns for TiO$_2$ based photocatalytic enhancement: suitable band gap value for higher efficiency of visible light absorption, higher carrier mobility for lower electron–hole recombination rate, and lower work function for redox reaction [15]. Besides controlling defect density that modulates the band gap, work function, and electroaffinity by atomic under coordination [16], doping is another effective means for such purpose by narrowing its band gap or introducing the impurity level (IL), it will reduce the energy required to excite electrons from valence band (VB) to conduction band (CB) effectively [17,18].

Nonmetal (C, N, B, etc.) [12,19–23] and transition metal (TM) (Ta, Ni, Mo, Nb, Fe, Cu, etc.) doped specimens [3,24–30] have been extensively studied both theoretically and experimentally. In previous studies, nonmetal doping influences the VB by affecting the O-2p electrons and extends the optical absorption edge of TiO$_2$ to visible light regime [3,31]. For instance, nitrogen addition enhances the responding to the visible light [23,32,33]; carbon addition raises the upper edge of VB and reduces the band gap [11]. On the other hand, metallic dopants introduce defects or distort the surrounding crystal structure which affects the CB through the interaction with Ti-3d orbitals, suppresses the recombination of electron–hole pairs and extends the optical response energy [3]. For instance, Ta ion favors to separate charge and effectively improve water splitting [29]; Nb dopant can effectively extend the absorption edge into visible light region and enhance the photocatalytic activity [34].

Researches indicated that TM-nonmetal co-doped specimen has better photocatalytic efficiency than single-doped specimen since the introduced metal ion will be a mediator for interfacial charge transfer in nonmetal doped specimen, which suppresses the recombination of electron–hole pairs. Thus, co-doping may combine the features of each dopant and promote the photocatalytic efficiency [35–37]. For example, Cheney et al. [38] reported that the band gap reduction and carrier delocalization in Cr–N co-doped TiO$_2$ are critical to efficient light-to-current conversion in oxide semiconductors. Run and co-workers [39] reported that the Ta–N co-doped TiO$_2$ can narrow the band gap of pure TiO$_2$ significantly by about 0.48 eV.
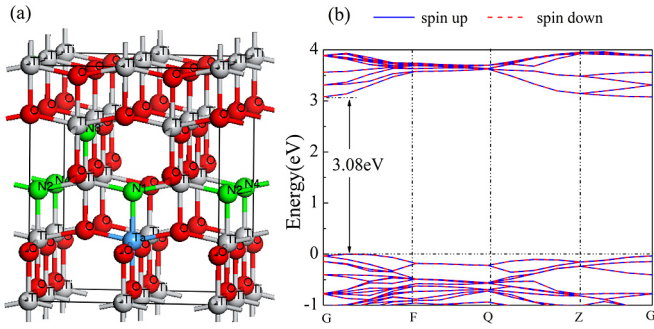
Fig. 1. (Color online.) (a) A 48-atom super-cell for the crystal structure of co-doped anatase TiO_2. The red, gray, green and blue atoms denote O, Ti, N and Ta, respectively. The number of 1, 2, 3 and 4 denote the different substituted positions of N atom. (b) Band structure of pure TiO_2, where the blue solid (red dashed) lines refer to the spin up (spin down) states.

Although the optical and photocatalytic activities of the doped TiO_2 specimens have been reported, and the variation of processing conditions shows profound influences on its semiconducting properties and photocatalytic performance [3], the fundamental understanding of the TM-nonmetal bonding is also ambivalent. In this study, we examine four co-doped specimens (Ta–N^1, Ta–N^2, Ta–N^3, Ta–N^4) with different Ta and N co-doped positions. A systematic study of the structural, electronic, optical and photocatalytic properties of N or Ta doped and Ta–N co-doped TiO_2 on basis of first principle calculations and experimental observations. The photocatalytic activity was tested by degrading the methylene blue (MB) under visible light.

2. Computational and experimental methods

All specimens with space group $I4_1/amd$ (see Fig. 1(a)) were built. The energy, crystal structure, partial density of states (PDOS) and band structure were calculated based on density functional theory with the Perdew–Burke–Ernzerhof functional of the generalized gradient approximation (GGA) [40] and norm-conserving pseudopotentials [41], as implemented in the CASTEP code. The cutoff kinetic energy with 750 eV and $5 \times 5 \times 4$ k-point sampling set were sufficiently large for the specimens considered. The convergence tolerance of maximum force, maximum displacement and energy were 0.01 eV/Å, 5.0×10^{-4} Å and 5.0×10^{-6} eV/atom, respectively. The GGA + U approach was considered the strongly correlated interactions of the Ti-3d orbitals, a moderate on-site coulomb repulsion $U = 7.0$ eV was applied, and the band gap 3.08 eV for pure TiO_2 is close to the experimental value 3.20 eV. Moreover, three kinds of super-cells ($Ti_{16}O_{31}N$, $Ti_{15}TaO_{32}$ and $Ti_{15}TaO_{31}N$) were built, where the Ta and N atoms substituted the Ti and O atoms, respectively. Based on the distance between Ta and N atoms, four co-doped specimens, labeled as Ta–N^1, Ta–N^2, Ta–N^3 and Ta–N^4, were considered as N atom located in four different positions (labeled as 1, 2, 3 and 4 in Fig. 1(a)).

The formation energies E_f of dopants were estimated to calculate the thermal stability of the doped specimens:

$$E_f = E(\text{doped}) - E(\text{pure}) + m\mu_{Ti} + n\mu_O - m\mu_{Ta} - n\mu_N \quad (1)$$

where $E(\text{doped})$ and $E(\text{pure})$ are the total energies of the doped and pure TiO_2. μ_{Ta} is the chemical potential of Ta from bulk atoms. [39] μ_N is the chemical potential of N that determined by the energy of the N_2 molecule [42,43]. The coefficients m and n are the numbers of Ta and N atoms doped into the supercells of TiO_2, respectively. The formation energy is not fixed but depends on the growth condition, which can be changed from Ti-rich to O-rich. Under the Ti-rich condition the μ_{Ti} is the chemical potential of Ti from bulk atoms, while the chemical potential of O is calculated

by the equation: $\mu_{Ti} + \mu_O = \mu(TiO_2)$. However, under O-rich condition, μ_O is the chemical potential of the ground-state energy of the O_2 molecule, while the chemical potential of Ti is also obtained by the equation: $\mu_{Ti} + 2\mu_O = \mu(TiO_2)$.

Titanium butoxide [$Ti(OC_4H_9)_4$] was used as a precursor to synthesize pure TiO_2 by sol–gel method using glacial acetic acid (HAc) as a catalyst. The molar ratio of $Ti(OC_4H_9)_4$/H_2O/ethanol/HAc was kept constant at 1/3.3/20.1/3.5. Pure TiO_2 sol was prepared by constantly stirring the precursor in ethanol for 30 minute at room temperature to obtain solution A. Then de-ionized water, ethanol and HAc were mixed together to form solution B. Urea (NH_2CONH_2) and tantalum pentachloride ($TaCl_5$) as sources of N and Ta dopants were interacted with solution A and B, respectively, keeping the molar ratio of (N or Ta)/Ti at 6.25%. Later, solution B was added dropwisely into solution A, and the resulting solution was then constantly stirred for 1 h at 25 °C to enhance its homogeneity. The obtained solutions were kept 24 h at 25 °C for ageing and then dried at 80 °C for 8 h to remove the excess solvents. After fully grinding, the resulting powders were calcinated in air at 500 °C for 1 h to obtain the final specimens.

The optical absorption curves of all specimens were measured by a Shimadzu UV 3600 spectrophotometer. X-ray diffraction (XRD) patterns were collected on a Bruker D2 Phaser diffractometer with Cu Kα radiation ($\lambda = 1.54056$ Å). Raman spectra were collected using a Renishaw inVia Reflex micro-Raman spectrometer. The X-ray photoelectron spectroscopy (XPS) measurements performed on a Thermo Scientific K-Alpha spectrometer with a monochromatic Al Kα X-ray source of 1486.6 eV. The photocatalytic activities were evaluated by measuring the absorbance of methylene blue (MB) degradation under visible light irradiation in aqueous solution. The 50 mg of photocatalyst was added into 50 ml of aqueous MB (5 mg/L) solution. Prior to irradiation, the suspensions were continuously stirred in a darkroom for 30 minutes to reach the adsorption–desorption equilibrium. The light source was a 500 W xenon lamp (JOYN-GHX-A) with a UV filter that can cut off the UV light. The lamp was cooled with flowing water to keep room temperature during the whole photocatalytic reaction. Aliquots were taken from the suspension per hour and immediately centrifuged, the MB concentrations were analyzed by a visible spectrophotometer (722S) and the adsorption peak at 664 nm was recorded.

3. Results and discussion

3.1. Structural properties and thermal stability

The XRD patterns of all specimens were shown in Fig. 2. Due to the (101), (112), (200), (105), (211) and (204) characteristic peaks, all specimens show the anatase phase and no reflection peaks induced by doping are detected. To confirm the impurities substitute in anatase phase, the Raman spectra were also taken. In Fig. 3, the Raman scattering peaks appearing at 145, 197, 398, 515 and 640 cm^{-1} are identified as $E_{g(1)}$, $E_{g(2)}$, $B_{1g(1)}$, $A_{1g} + B_{1g(2)}$ and $E_{g(3)}$ vibration modes of anatase phase [44], these are without presence of the reflection peaks due to doping. The Raman observation is consistent with the XRD results, and thus the TM oxides clusters are not exist in the specimens. The inserted image shown the first scattering peaks ($E_{g(1)}$ at 145 cm^{-1}) with normalized intensity. It is found that, the peak position of all doped TiO_2 are invariable, compared with pure TiO_2, the peak width remains constant for N-doped specimen but widen for Ta-doped and Ta–N co-doped specimens.

Our calculated lattice constants of pure TiO_2 are $a = b = 7.606$ Å and $c = 9.567$ Å (Table 1), which agree with the previously reported experimental values ($a = b = 7.568$ Å, $c = 9.515$ Å) [45] and calculated values ($a = b = 7.532$ Å, $c = 9.637$ Å) [46]. The lattice deformations are less than 1.0% in a and b axis and 0.6%